

# Mechanism of asymmetric photocyclization of $\alpha$ -oxoamides

Daisuke Hashizume,<sup>a</sup> Hidenori Kogo,<sup>a</sup> Akiko Sekine,<sup>a</sup> Yuji Ohashi,<sup>\*,a</sup> Hisakazu Miyamoto<sup>b</sup> and Fumio Toda<sup>b</sup>

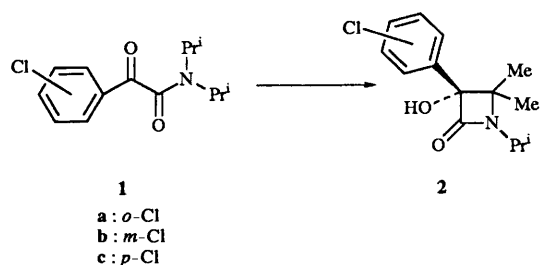
<sup>a</sup> Department of Chemistry, Tokyo Institute of Technology, Ookayama, Meguro-ku, Tokyo 152, Japan

<sup>b</sup> Department of Applied Chemistry, Ehime University, Bunkyo, Ehime 790, Japan

The molecules of *N,N*-diisopropylarylglyoxylamides, **1**, are converted into the corresponding  $\beta$ -lactams, **2**, on exposure to UV light in the solid state. However, the chemical and optical yields of the photocyclization are quite different among the crystals. The crystal structures of the three positional isomers **1a–c** as reactants and the photoproduct **2b** derived from **1b** are determined by X-ray structure analysis: (**1a**) *o*-chlorophenyl-*N,N*-diisopropylglyoxylamide; (**1b**) *m*-chlorophenyl-*N,N*-diisopropylglyoxylamide; (**1c**) *p*-chlorophenyl-*N,N*-diisopropylglyoxylamide; (**2b**) 3-(*m*-chlorophenyl)-3-hydroxy-*N*-isopropyl-4,4-dimethylazetidin-2-one. The reactivity and enantioselectivity of the reactions are discussed on the basis of the structures and the packing potential energy calculated.

Optically active  $\beta$ -lactams are important antibiotics, and have long been a target of organic synthesis. In all cases, however, a chiral source is essential for enantiomeric control. It has been found that the achiral molecules of *N,N*-diisopropylphenylglyoxylamide **1d** crystallize in a chiral space group and are transformed to optically almost pure  $\beta$ -lactam when the powdered sample is irradiated with UV light.<sup>1</sup>

Although the structures of the reactant glyoxylamide and the produced  $\beta$ -lactam were determined by X-ray structure analysis, the mechanism of asymmetric induction was not clarified since the absolute configurations of the reactant and product crystals were not determined.<sup>2</sup> Recently three glyoxylamide molecules which have chlorine atoms as phenyl substituents were synthesized to elucidate the process of asymmetric photocyclization. This paper reports the molecular and crystal structures of these three glyoxylamides **1a–c** and the photoproduct **2b**, derived from **1b**, and discusses the mechanism of the asymmetric photocyclization.



## Results and discussion

### Crystal and molecular structure

The crystal structure of **1a** viewed along the *a*-axis is shown in Fig. 1. There are no unusually short contacts between the molecules. The molecular structure is shown in Fig. 2 with the numbering of the atoms. Selected bond distances and angles are listed in Table 1. The amide moiety is planar within 0.08 Å and the carbonyl group of the benzoyl moiety is almost perpendicular to the amide moiety. The torsion angles of O(1)–C(7)–C(8)–O(2) and C(7)–C(8)–N(1)–C(9) are 107.8(8) and –15.8(8)°, respectively. The above conformation allows some intramolecular short contacts. The distances of C(7)···C(9) and O(1)···H(9) are 2.889(9) and 2.65(5) Å, respectively. These distances are significantly shorter than the sum of the van der Waals radii of the corresponding atoms (3.50 and 2.95 Å).<sup>3</sup> Such

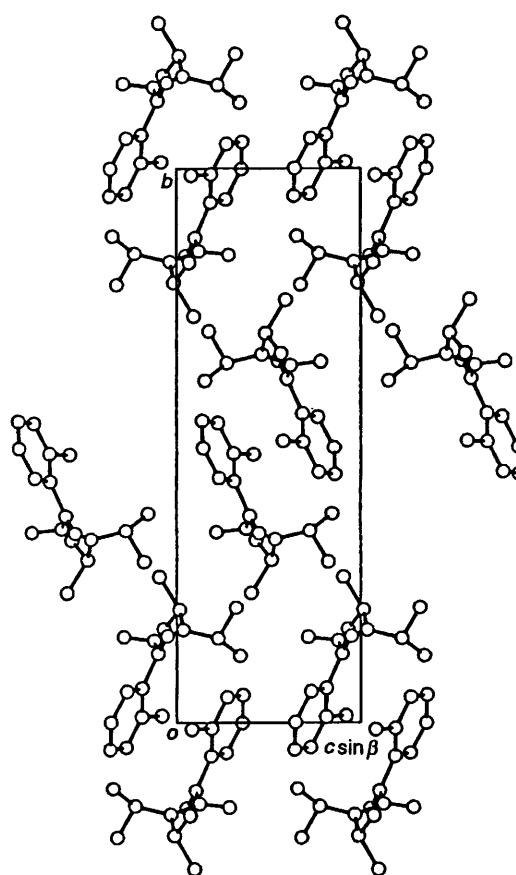


Fig. 1 Crystal structure of **1a** viewed along the *a*-axis

short contacts are also evident in the structure of **1d**, with corresponding distances of 2.871(5) and 2.78(5) Å.<sup>2</sup>

Figs. 3 and 4 show the crystal structures of **1b** and **1c** viewed along the *c*-axis. There are no unusually short contacts between the molecules in either structure. The molecular structures of **1b** and **1c** are shown in Figs. 5 and 6, respectively, with the numbering of the atoms. Selected bond distances and angles of **1b** and **1c** are also listed in Table 1. The molecular structures of **1b** and **1c** are essentially the same as that of **1a**. The torsion angles of O(1)–C(7)–C(8)–O(2) and C(7)–C(8)–N(1)–C(9) are 87.1(9) and –5(1) and 99.6(5) and –5.4(5)° for **1b** and **1c**

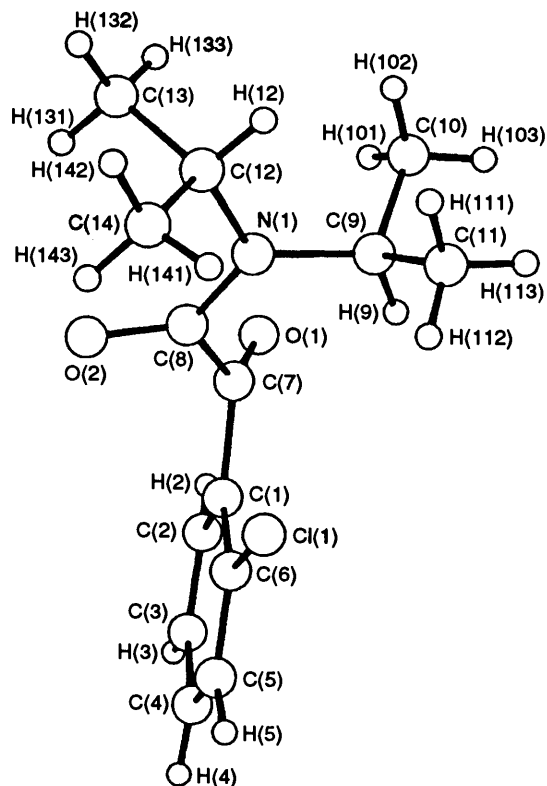


Fig. 2 Molecular structure and numbering of atoms of **1a**

Table 1 Selected bond distances (Å) and angles (°) for **1a–c**

	<b>1a</b>	<b>1b</b>	<b>1c</b>
O(1)–C(7)	1.148(6)	1.204(8)	1.217(4)
O(2)–C(8)	1.232(7)	1.240(8)	1.234(4)
N(1)–C(8)	1.354(7)	1.306(8)	1.333(4)
N(1)–C(9)	1.468(7)	1.508(9)	1.486(5)
N(1)–C(12)	1.478(6)	1.490(9)	1.491(5)
C(1)–C(7)	1.511(7)	1.490(9)	1.486(5)
C(7)–C(8)	1.556(8)	1.521(9)	1.518(5)
C(8)–N(1)–C(9)	121.0(6)	120.6(6)	120.8(3)
C(8)–N(1)–C(12)	120.0(5)	121.4(6)	120.3(3)
C(9)–N(1)–C(12)	119.0(5)	118.1(6)	118.8(3)
O(1)–C(7)–C(1)	119.9(6)	122.0(7)	122.6(4)
O(1)–C(7)–C(8)	121.7(6)	120.3(6)	118.9(4)
C(1)–C(7)–C(8)	117.3(6)	117.3(6)	118.3(3)
O(2)–C(8)–N(1)	124.8(7)	125.6(7)	125.4(4)
O(2)–C(8)–C(7)	115.6(6)	115.0(7)	115.6(4)
N(1)–C(8)–C(7)	119.0(6)	119.4(7)	118.9(4)

respectively. The intramolecular distances of C(7)···C(9) and O(1)···H(9) are 2.82(1) and 2.75(7) Å for **1b** and 2.83(1) and 2.55(4) Å for **1c**, respectively. These are significantly shorter than the sum of the van der Waals radii.

Fig. 7 shows the crystal structure of **2b** viewed along the *b*-axis. There are two crystallographically independent molecules, which are related by a pseudo-inversion centre. The intermolecular hydrogen bonds are formed between the hydroxy groups and the oxygen atoms of the carbonyl groups, O(1A)–H(9A)···O(2A) and O(1B)–H(9B)···O(2B). The molecules A and B are linked along the *z* axis by the hydrogen bonds. The bond lengths of O(1A)···O(2A), H(9A)···O(2A), O(1B)···O(2B) and H(9B)···O(2B) are 2.708(7), 1.80, 2.692(9) and 1.54 Å, respectively. The corresponding angles for O(1A)–H(9A)···O(2A) and O(1B)–H(9B)···O(2B) are 168 and 166°, respectively.

The molecular structures of molecules A and B of **2b** are shown in Figs. 8(a) and (b) with the numbering of the atoms. Although both of the structures have disordered isopropyl

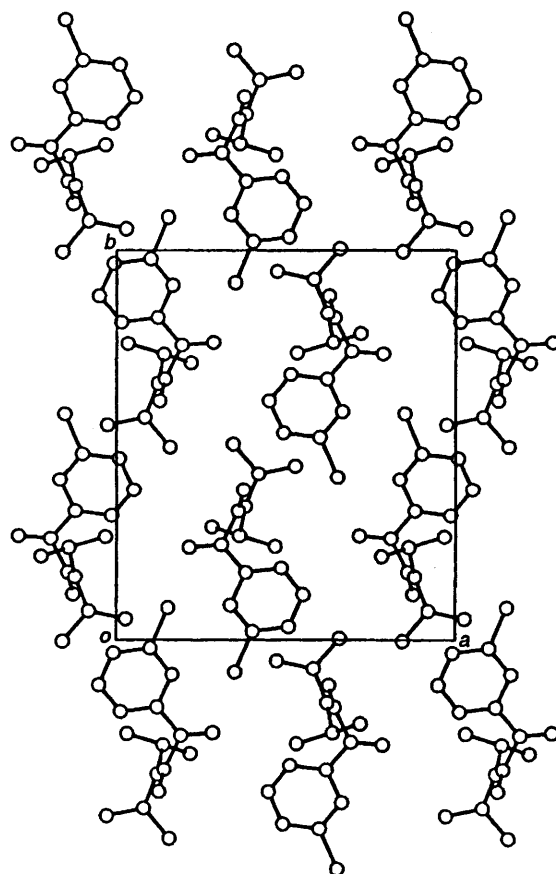


Fig. 3 Crystal structure of **1b** viewed along the *c*-axis

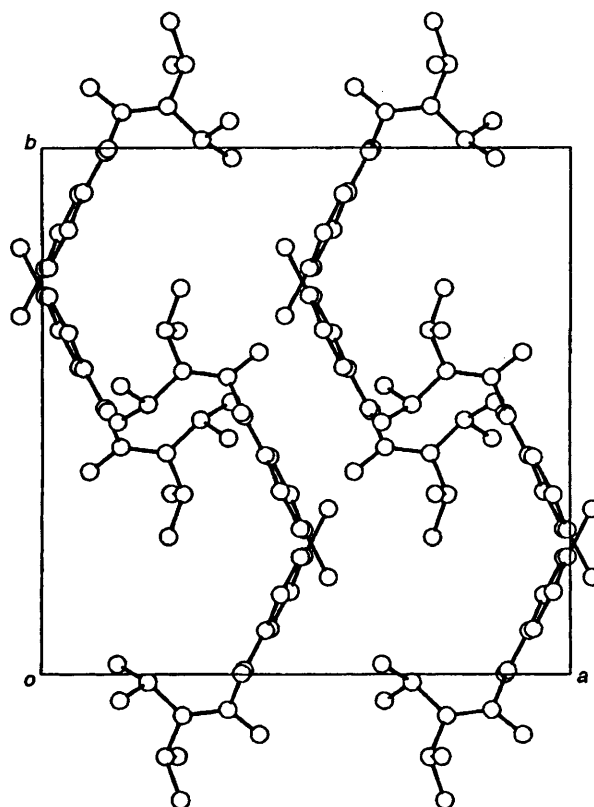


Fig. 4 Crystal structure of **1c** viewed along the *c*-axis

groups bonded to the nitrogen, only major parts are drawn. The absolute configuration of the chiral carbon, C(7), is *S* for both molecules. Selected bond distances and angles are listed in

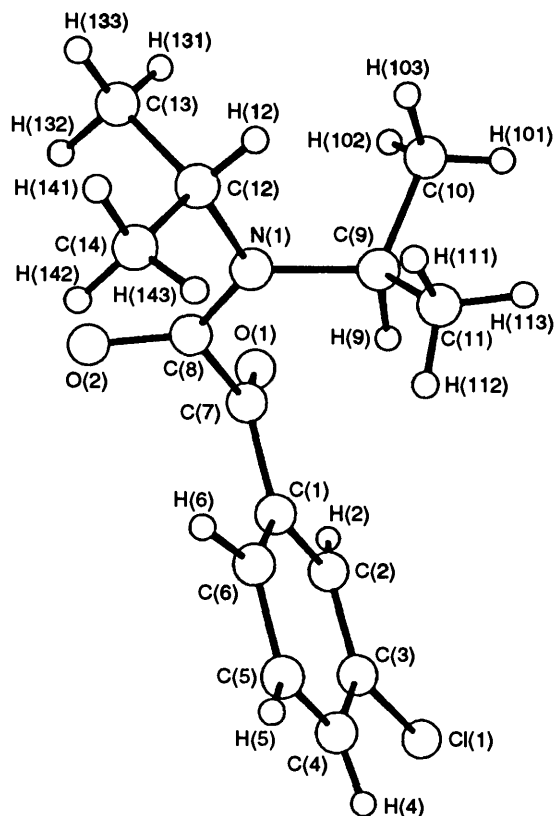


Fig. 5 Molecular structure and numbering of atoms of **1b**

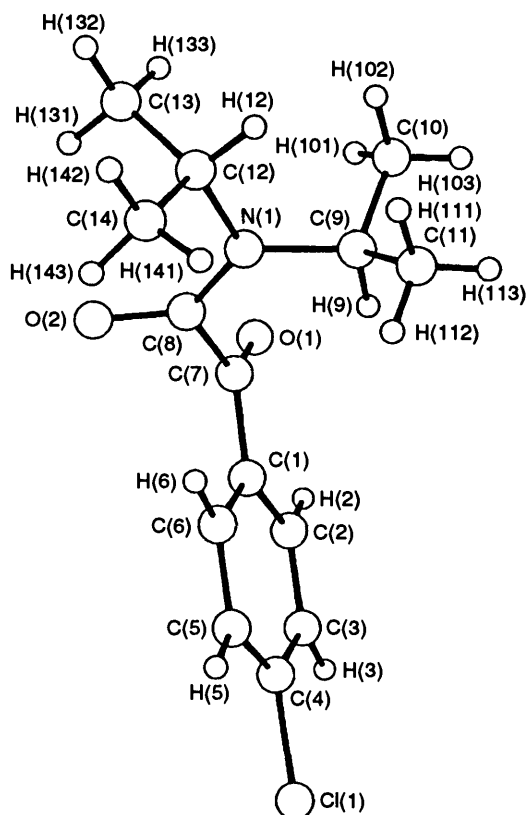


Fig. 6 Molecular structure and numbering of atoms of **1c**

Table 2. The structures of the two molecules are very similar to each other. The bond distances of C(7A)–C(9A) and C(7B)–

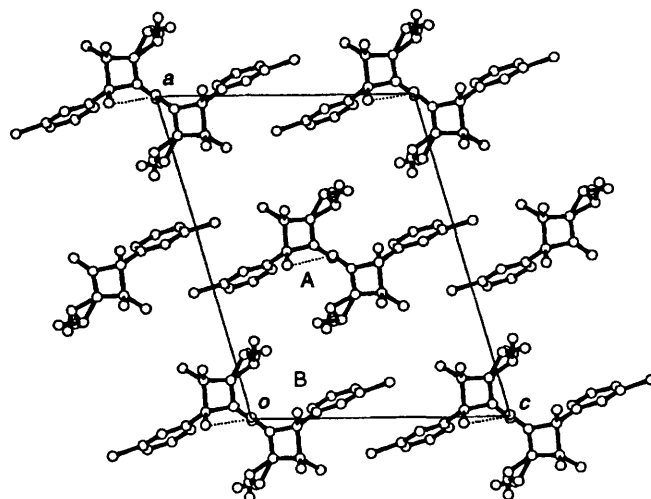


Fig. 7 Crystal structure of **2b** viewed along the *b*-axis

C(9B) are elongated by the steric repulsion between the bulky substituents.

### Mechanism of asymmetric reaction

When the crystal is irradiated with UV light, a radical is probably produced at the oxygen, O(1), of the carbonyl group. The produced oxygen radical should abstract the hydrogen atom H(9) of the isopropyl group to form a hydroxy group. The radical produced at C(9) due to the abstraction of H(9) would then attack the C(7) atom to form a C–C single bond. This forms a  $\beta$ -lactam ring as shown in Fig. 9. The intramolecular short contacts between O(1)···H(9) and C(7)···C(9) in all the three crystals support the above mechanism, which has already been proposed in a previous paper.<sup>2</sup>

The absolute structures of the **1b** and **2b** in Fig. 9 are in agreement with those determined with anomalous dispersion terms for the chlorine atoms. If the radical C(9) attacks the atom C(7) from the *si*-face of the carbonyl group as shown in Fig. 9, the produced  $\beta$ -lactam should have the *S* configuration, which is in agreement with the experimental result. This clearly indicates that the photocyclization occurs topochemically.

This mechanism also explains why racemic  $\beta$ -lactams were produced from the crystals of **1a** and **1c**. Since both crystals have a centre of symmetry, both chiral environments for the starting material exist in the crystals. This brings about the racemic product after the photocyclization.

### Difference in reactivity

Although the three glyoxylamides, **1a–c**, have almost identical structures, the reaction yields differ for the three crystals as shown in Table 3. This may be due to the difference in the conformation of the aryl group, since the other structural parameters are almost the same for the three crystals. Moreover, the orientation of the aryl group seems to play an important role in the reaction, since the aryl group must approach close to the isopropyl group, and the rotation of the aryl group around the C(1)–C(7) bond is necessary to avoid the steric repulsion between these two bulky groups.

For the *m*-Cl derivative **1b**, which showed the highest reaction yield, the torsion angle of C(6)–C(1)–C(7)–C(8) in **1b** is  $1(1)^\circ$  whereas the corresponding angles in **2b** are  $-7(1)$  and  $-10(1)^\circ$  for molecules A and B, respectively. This suggests that the aryl group should rotate around the C(1)–C(7) bond by  $-8$  or  $-11^\circ$  to take the conformation of the molecules A or B in **2b**, respectively.

The repulsive energy for rotation about the C(1)–C(7) bond in

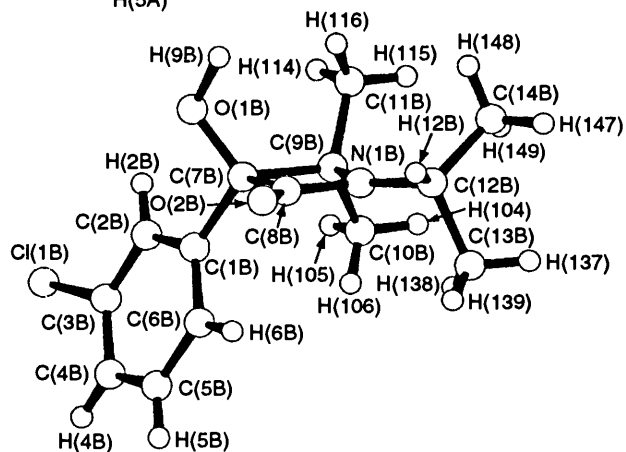
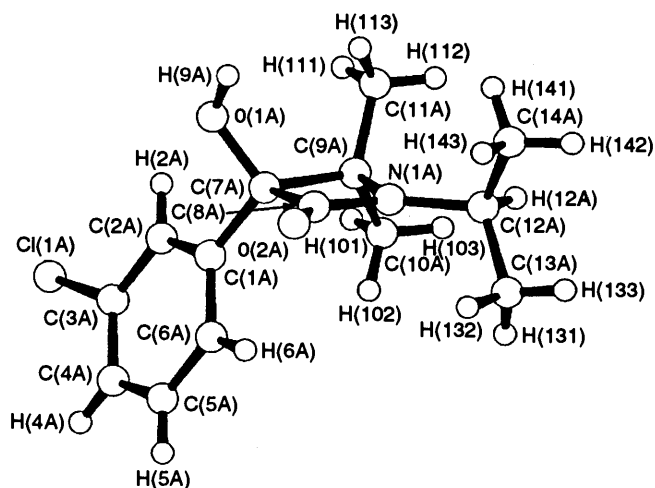


Fig. 8 Molecular structures and numberings of atoms (a) for A and (b) for B, respectively, of **2b**

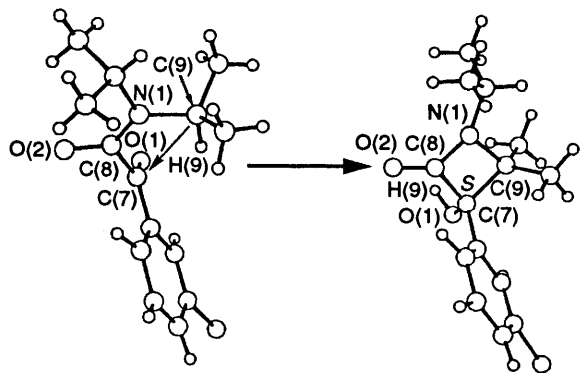


Fig. 9 The process of the reaction

the crystal structure of **1b** was calculated using the program OPEC.<sup>4</sup> Fig. 10 shows the intra- and inter-molecular potential energies *vs.* the rotation of the aryl group around the C(1)–C(7) bond. If we assume that the crystal structure is retained during the reaction, the repulsive energy increases only 0.4 or 1.7 kcal mol<sup>-1</sup>† for the conformation of the molecules A or B, respectively. On the other hand, for the *o*-Cl derivative **1a**, which showed the lowest chemical yield (42%), the torsion angle of C(6)–C(1)–C(7)–C(8) is –36.7(8)°. Unfortunately we had no crystals of **2a** suitable for the X-ray analysis. Molecular structures were calculated with the program MOPAC,<sup>5</sup> starting from model structures with the same conformations as molecules A and B of **2b**. The torsion angles of C(6)–C(1)–C(7)–

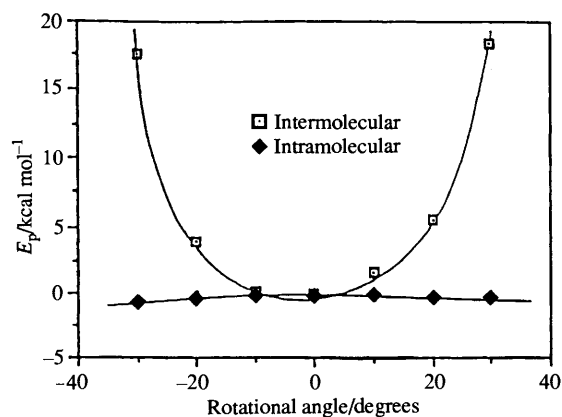


Fig. 10 The potential of energies for steric repulsion against the rotation of aryl group for **1a**

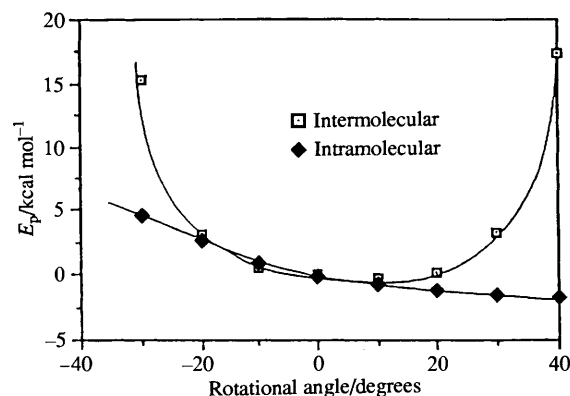


Fig. 11 The potential of energies for steric repulsion against the rotation of aryl group for **1b**

Table 2 Selected bond distances (Å) and angles (°) for **2b**

	Molecule A	Molecule B
O(1)–C(7)	1.402(9)	1.399(11)
O(2)–C(8)	1.22(1)	1.22(1)
N(1)–C(8)	1.33(1)	1.34(1)
N(1)–C(9)	1.49(1)	1.50(1)
C(1)–C(7)	1.50(1)	1.52(1)
C(7)–C(8)	1.53(1)	1.54(1)
C(7)–C(9)	1.57(1)	1.61(1)
C(8)–N(1)–C(9)	96.6(6)	97.0(7)
O(1)–C(7)–C(1)	106.2(6)	107.6(7)
O(1)–C(7)–C(8)	113.8(6)	115.5(7)
O(1)–C(7)–C(9)	115.6(7)	116.8(8)
C(1)–C(7)–C(8)	118.3(7)	116.2(9)
C(1)–C(7)–C(9)	116.8(7)	114.6(7)
C(7)–C(9)–C(10)	117.5(7)	117.1(8)
C(7)–C(9)–C(11)	114.7(8)	112.1(10)
C(10)–C(9)–C(11)	111.8(9)	113.2(10)
O(2)–C(8)–N(1)	132.8(8)	133.5(9)
O(2)–C(8)–C(7)	134.8(8)	133.3(10)
N(1)–C(8)–C(7)	92.4(7)	93.1(8)

Table 3 The results of the photoreaction

Reactant	Chemical yield (%)	Optical yield (%ee)
<b>1a</b>	42	—
<b>1b</b>	75	100 <sup>a</sup>
<b>1c</b>	50	—

<sup>a</sup> [ $\alpha$ ]<sub>D</sub> –106 (*c* 0.84, CHCl<sub>3</sub>). The optical purity of **2b** was determined by HPLC on an optically active solid phase, Chiralcel OC of Daicel Chemical Industries, Ltd., Himeji, Japan.

† 1 cal = 4.184 J.

**Table 4** Crystal data and experimental conditions

	<b>1a</b>	<b>1b</b>	<b>1c</b>	<b>2b</b>
Chemical formula			C <sub>14</sub> H <sub>18</sub> NO <sub>2</sub> Cl	
Formula weight			267.76	
Crystal system	Monoclinic	Orthorhombic	Orthorhombic	Monoclinic
Space group	<i>P</i> 2 <sub>1</sub> / <i>n</i>	<i>P</i> 2 <sub>1</sub> 2 <sub>1</sub> 2 <sub>1</sub>	<i>Pbca</i>	<i>P</i> 2 <sub>1</sub>
<i>Z</i>	4	4	8	4
<i>a</i> /Å	9.582(1)	12.800(3)	15.177(1)	17.125(3)
<i>b</i> /Å	21.494(1)	14.941(1)	15.558(1)	6.914(1)
<i>c</i> /Å	7.591(1)	7.611(1)	12.555(1)	13.030(1)
$\beta$ /°	111.40(1)	—	—	106.124(5)
<i>V</i> /Å <sup>3</sup>	1455.6(3)	1455.6(5)	2964.6(2)	1482.2(3)
<i>D<sub>x</sub></i> /Mg m <sup>-3</sup>	1.222	1.222	1.200	1.200
Diffractometer			AFC-4	
Radiation			Cu-K $\alpha$	
$\lambda$ /Å			1.541 84	
$\mu$ (Cu-K $\alpha$ )/mm <sup>-1</sup>	2.300	2.300	2.259	2.133
<i>F</i> (000)	568	568	1 136	568
Crystal dimensions/mm <sup>3</sup>	0.3 × 0.2 × 0.2	0.4 × 0.2 × 0.2	0.5 × 0.4 × 0.3	0.5 × 0.2 × 0.2
<i>T</i> /K			296	
2 $\theta$ <sub>max</sub> /°			125	
Range of <i>h</i> , <i>k</i> and <i>l</i>	-13 ≤ <i>h</i> ≤ 13 -26 ≤ <i>k</i> ≤ 0 0 ≤ <i>l</i> ≤ 10	0 ≤ <i>h</i> ≤ 17 0 ≤ <i>k</i> ≤ 19 0 ≤ <i>l</i> ≤ 11	0 ≤ <i>h</i> ≤ 18 0 ≤ <i>k</i> ≤ 18 0 ≤ <i>l</i> ≤ 15	-22 ≤ <i>h</i> ≤ 22 -10 ≤ <i>k</i> ≤ 0 0 ≤ <i>l</i> ≤ 17
Scan technique			$\omega$ -2 $\theta$	
Scan width/°			1.0 + 0.15tan $\theta$	
Scan rate/°(2 $\theta$ ) min <sup>-1</sup>			8	
Independent reflections	2 231	1 382	2 694	2 570
Observed reflections	1 338	1 239	1 614	1 861
	<i>I</i> > 3 $\sigma$ <i>I</i>	<i>I</i> > 3 $\sigma$ <i>I</i>	<i>I</i> > 3 $\sigma$ <i>I</i>	<i>I</i> > 0
<i>R</i> ( <i>F</i> )	0.070	0.064	0.062	0.061
<i>wR</i> ( <i>F</i> )	0.050	0.064	0.046	—
<i>wR</i> ( <i>F</i> <sup>2</sup> )	—	—	—	0.158
<i>S</i>	4.15	7.24	4.13	1.20
Extinction coefficient	—	—	—	0.001 742
( $\Delta$ / $\sigma$ ) <sub>max</sub>	0.01	0.06	0.01	0.00
$\Delta\rho$ /e Å <sup>-3</sup>	-0.25, 0.25	-0.30, 0.42	-0.24, 0.31	-0.19, 0.22

C(8) became +1.4 and -7.0° for the two starting models, A and B, respectively. This suggests that a rotation of -38.1 or -29.7° around the C(1)-C(7) bond is necessary in the process of the photocyclization. The repulsive energy *vs.* the rotation around the C(1)-C(7) bond was calculated for the crystal of **1a**, which is shown in Fig. 11. The repulsive energy increases significantly for both models. Since the crystal structure may be destroyed in the process of the photoreaction, the above calculation may only be the first approximation. However, the difference in torsional change should play an important role in this photocyclization.

### Experimental

Photoreaction of the three glyoxylamides was carried out as follows. One single crystal of glyoxylamide, **1**, was cut into two pieces. One piece was ground to a powder and irradiated for 10 h with a 400 W high-pressure mercury lamp. Only crystals of **1b** gave optically active  $\beta$ -lactam, **2b**, which has a negative optical rotation. The others gave racemic products. By seeding with finely powdered crystals from another piece of crystal during recrystallization of **1b** from methanol, crystals which give (-)-**2b** were prepared in a large quantity. To obtain quantitative values of the chemical and optical yields, a large amount of crystals was prepared for the photoreaction. The powdered crystals of **1** were irradiated with the mercury lamp. The chemical and optical yields were determined after purification by column chromatography. The results are summarized in Table 3.

The crystal data and experimental details of **1a-c** and **2b** are summarized in Table 4. The Lorentz, polarization and decay corrections were applied for all the crystals, and an extinction correction was applied for **2b**. The structures were solved by

direct methods, using the program MITHRIL<sup>6</sup> for **1a-c** and SIR-92<sup>7</sup> for **2b**. The structures were refined by the full-matrix least-squares method with the program TEXSAN<sup>8</sup> for **1a-c** and SHELXL-93<sup>9</sup> for **2b**. The weighting schemes were  $w = [\sigma(F_o)^2]^{-1}$  for **1a-c** and  $w = [\sigma(F_o^2)^2 + (0.0801 P)^2 + 0.3634 P]^{-1}$ , where  $P = (F_o^2 + 2F_c^2)/3$ , for **2b**. Both of the crystallographically independent isopropyl groups bonded to the nitrogen atoms are disordered in **2b**. The occupancy factors were also refined to have the same isotropic temperature factors. The positions of several hydrogen atoms were obtained on difference maps and refined isotropically. The other hydrogen atoms were calculated geometrically and not refined. The anisotropic temperature factors were applied to all non-hydrogens except the disordered atoms in the final refinement. Atomic scattering factors were taken from the International Tables for X-Ray Crystallography.<sup>10</sup> The absolute structures of **1b** and **2b** were determined by the anomalous scattering of Cu-K $\alpha$  radiation.

### Acknowledgements

This work was partly supported by a Grant-in-Aid for Scientific Research from the Ministry of Education, Science and Culture, Japan.

### References

- 1 F. Toda, M. Yagi and S. Soda, *J. Chem. Soc., Chem. Commun.*, 1987, 1413.
- 2 A. Sekine, K. Hori, Y. Ohashi, M. Yagi and F. Toda, *J. Am. Chem. Soc.*, 1989, **111**, 697.
- 3 A. Bondi, *J. Phys. Chem.*, 1964, **68**, 443.
- 4 A. Gavezzotti, *J. Am. Chem. Soc.*, 1991, **113**, 4622.

- 5 J. J. P. Stewart, *MOPAC QCPE*, Program 455 (version 3), University of Indiana, USA, 1983.
- 6 G. J. Gilmore, *J. Appl. Crystallogr.*, 1984, **17**, 42.
- 7 G. Cascarano, C. Giacovazzo, A. Guagliardi, M. C. Burla, G. Polidori and M. Camalli, *J. Appl. Crystallogr.*, 1994, **27**, 435.
- 8 Molecular Structure Corporation, TEXSAN, Single Crystal Structure Analysis Software Version 5.0, 1989.
- 9 G. M. Sheldrick, SHELXL-93, Program for the Refinement of the Crystal Structure, University of Goettingen, Germany, 1993.
- 10 *International Tables for X-Ray Crystallography*, Kynoch, Birmingham, 1974, vol. IV.

*Paper 5/03770K*  
*Received 12th June 1995*  
*Accepted 10th July 1995*